Domain Dynamics under Ultrafast Electric-Field Pulses

Tiannan Yang[1],[*] Bo Wang[1] Jia-Mian Hu[1,2] and Long-Qing Chen[1],[†]

[1]*Department of Materials Science and Engineering, The Pennsylvania State University,*
University Park, Pennsylvania 16802, USA
[2]*Department of Materials Science and Engineering, University of Wisconsin-Madison, Madison, Wisconsin 53706, USA*

Exploring the dynamic responses of a material is of importance to both understanding its fundamental physics at high frequencies and potential device applications. Here we develop a phase-field model for predicting the dynamics of ferroelectric materials and study the dynamic responses of ferroelectric domains and domain walls subjected to an ultrafast electric-field pulse. We discover a transition of domain evolution mechanisms from pure domain growth at a relatively low field to combined nucleation and growth of domains at a high field. We derive analytical models for the two regimes which allow us to extract the effective mass and damping coefficient of ferroelectric domain walls. The exhibition of two regimes for the ferroelectric domain dynamics at low and high electric fields is expected to be a general phenomenon that would appear for ferroic domains under other ultrafast stimuli. The present Letter also offers a general framework for studying domain dynamics and obtaining fundamental properties of domain walls and thus for manipulating the dynamic functionalities of ferroelectric materials.

Understanding the ultrafast dynamics of functional materials is an important research topic for both fundamental physics and exploring device applications and has garnered much interest in recent years [1–9]. New dynamic phenomena and responses of ferroelectric materials under ultrafast external stimuli (e.g., pulses or ac fields) have been discovered, e.g., the excitation of GHz lattice oscillations [10,11], the emergence of new transient phases [12,13], and unusual enhancement of multifunctional responses [14–16], which are absent in experiments at longer timescales. Theoretical understandings on various ultrafast ferroelectric phenomena were also developed using analytical models [17–25] for simple systems at the continuum scale as well as atomistic simulations [26–37] for more complex systems at the atomic scale. Mesoscale models incorporating nanoscale dynamics within complex ferroelectric domain structures while computationally viable to possible larger system scales (e.g., $\sim\mu$m), however, have not been established.

In this Letter, we extend the phase-field description of ferroelectric materials [38] to ultrafast timescales through integrating proper polarization dynamics and elastodynamics, which yields full spatiotemporal profiles of GHz-THz dynamics of ferroelectric and ferroelastic domains while taking into account the mesoscale domain and wall configurations involving elastic and electrostatic interactions. As an example, we study the responses of domains and domain walls in $BaTiO_3$ crystals to ultrafast electric-field pulses. We model the domain wall dynamics at different magnitudes of the applied electric field and develop analytical models for the domain wall motion

and domain switching as a function of the applied field pulse. Based on the simulation results and analytical models, we extract effective mass and damping coefficients of domain walls. We also construct a domain diagram summarizing the stable domain states as a function of the strength and duration of the pulsed field.

In a phase-field model, a ferroelectric domain structure is described by a combination of the spatial distributions of the polarization and strain fields. Existing phase-field models of ferroelectric domain evolution employ the time-dependent Ginzburg-Landau equation [39,40] for the relaxational kinetics of polarization towards equilibrium while assuming instantaneous mechanical equilibrium for the strains. Since these models neglect the inertia and momentum of domain evolution, they cannot properly describe the structural oscillations which exist typically within GHz-THz frequencies [10,11]. Our analysis of a single domain under an ac field (see Note S1 of the Supplemental Material [41]) demonstrates that the relaxational equation for the polarization is no longer valid for transient processes with a characteristic time $t < 100$ ns or dynamics under ultrafast stimuli with a duration or period $T < 100$ ns. Similarly, the mechanical equilibrium is usually assumed to be established much faster than polarization evolution, which may not be valid if the external stimuli are at GHz or higher frequencies. For example, if we approximate the time that a domain structure takes to establish its mechanical equilibrium as the time required for the propagation of mechanical waves across the whole dimension of the domain structure with the speed of sound (10^3–10^4 m/s in typical solids), the time scale for

establishing mechanical equilibrium is 10–100 ps for a domain size of 100 nm, comparable to the time scale of ultrafast processes. To capture the domain dynamics under ultrafast stimuli, we extend the phase-field model by coupling the dynamic equation for polarization $\mathbf{P}(\mathbf{x}, t)$ and the elastodynamics equation for mechanical displacement $\mathbf{u}(\mathbf{x}, t)$,

$$\mu_{ij}\frac{\partial^2 P_i}{\partial t^2} + \gamma_{ij}\frac{\partial P_i}{\partial t} + \frac{\delta F}{\delta P_j} = 0, \qquad (1)$$

$$\rho\frac{\partial^2 u_i}{\partial t^2} = f_{Vi} + \frac{\partial}{\partial x_j}\left(\sigma_{ij} + \beta\frac{\partial\sigma_{ij}}{\partial t}\right). \qquad (2)$$

$\boldsymbol{\mu}$ and $\boldsymbol{\gamma}$ are the mass and damping coefficients of polarization evolution. ρ, β, and $\mathbf{f}_V$ are the material density, the stiffness damping coefficient, and the external body force density, respectively. $\sigma_{ij} = c_{ijkl}(\varepsilon_{kl} - \varepsilon_{kl}^0)$ is the stress, where $\mathbf{c}$ is the stiffness tensor, $\boldsymbol{\epsilon}$ is the strain, and $\varepsilon_{ij}^0 = Q_{ijkl}P_kP_l$ is the eigenstrain arising from electromechanical coupling ($\mathbf{Q}$ being the electrostrictive tensor). For BaTiO$_3$, $\mu_{11} = 5 \times 10^{-11}$ J m/A^2, $\gamma_{11} = 5 \times 10^{-2}$ J m/(A^2 s) [11], $\rho = 6.02 \times 10^3$ kg/m^3, and $\beta = 6.0 \times 10^{-12}$ s. The free energy F and other material constants are from Refs. [42,43]. We develop numerical solutions to Eqs. (1) and (2) based on the semi-implicit Fourier-spectral method [44–46] (see Notes S2–S5 of the Supplemental Material [41]). Treatment of the thermal fluctuation is described in Note S6 of the Supplemental Material. It is noted that similar second-order polarization dynamics have been adopted in several existing Ginzburg-Landau models [22,47,48]. Very recently, we showed that the polarization dynamics given by Eq. (1) successfully captured the light-activated structural dynamics in BaTiO$_3$ by comparing with experimental measurements [11].

We employ an ultrafast electric-field pulse to excite the dynamic responses of ferroelectric domains and domain walls. As shown in Fig. 1(a), a BaTiO$_3$ crystal contains 90° a-c ferroelectric domain walls with a domain size of 300 nm and a spontaneous polarization $P_S = 0.26$ C/m^2 of each domain. We apply an electric-field pulse $E = 1$ MV/m parallel to the polarization in c domains with a duration of 5 ns. The polarization responses ΔP_3 are shown in the first panel of Fig. 1(b), indicating that the c domain undergoes a longitudinal polarization oscillation while the a domain experiences a polarization rotation towards the field direction. Due to the larger transverse dielectric permittivity than the longitudinal one, the ΔP_3 response in the a domain is much stronger than that in the c domain. Upon turning off the field, ΔP_3 instantly shows a reversed change and eventually reaches equilibrium at $\Delta P_3 \approx 0$; i.e., the polarization of each domain is mostly recovered.

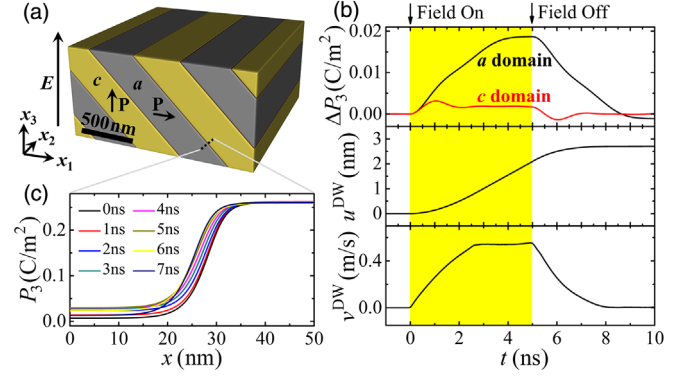At the meantime, a sideways motion of the a-c domain wall takes place with the c domain expanding into the

FIG. 1. (a) Schematic of a BaTiO$_3$ crystal with a-c domains subjected to an ultrafast electric-field pulse. (b) Evolution of (first panel) the polarization change of each domain as well as (second panel) the displacement and (third panel) the velocity of the sideways motion of the a-c domain wall, under an electric-field pulse $E = 1$ MV/m with duration indicated by the yellow region. (c) Evolution of the polarization profile across an a-c domain wall.

neighboring a domain, as shown in Fig. 1(c) for the evolution of polarization profile across the domain wall. The time-dependent *domain wall* (DW) displacement u^{DW} and velocity v^{DW} are shown in the second and third panels of Fig. 1(b). The domain wall shifts by a total of 2.7 nm in the whole process. The domain wall velocity undergoes a rise stage before reaching a maximum of 0.5 m/s at $t \approx 2.5$ ns, followed by a decay stage till $t \approx 8$ ns after turning off the electric field. Such rise and decay stages of domain wall motion as well as the polarization oscillation in c domains can only be revealed by a dynamical phase-field model and are absent in relaxational phase-field simulations (see Note S7 of the Supplemental Material [41]).

We next study the effects of the strength and duration of the electric-field pulses on the domain and domain wall dynamics. It is found that the domain evolution mechanisms are different for different ranges of the electric field strength: $E \leq 2$ MV/m, referred to as low field and $E > 2$ MV/m, referred to as high field. Under low fields, the domain structure exhibits pure domain growth dynamics with c domains expanding towards a domains through sideways motion of the a-c domain walls, without altering the overall domain pattern. Figure 2(a) presents the volume fraction ΔV^a of switched a domains under low fields as a function of pulse duration T_E. ΔV^a shows an almost linear dependence on both the pulse duration and the field strength.

To understand this relation, we analyze the domain wall velocity under a static electric field, as shown in Fig. 2(b). It is found that the dynamics of the domain wall almost perfectly resembles the motion of a particle with an effective mass m^{DW} and an effective damping coefficient α^{DW}; i.e., the displacement $u^{\text{DW}}(t)$ of the domain wall follows an analytical description
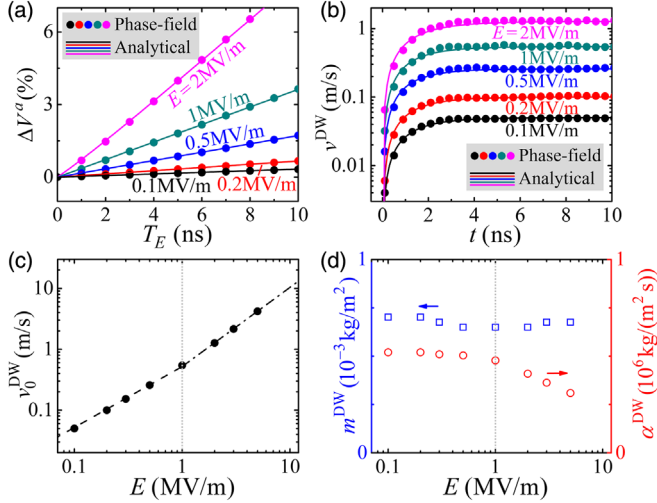
FIG. 2. (a) Volume fraction of switched a domains under low fields as a function of pulse duration, from both the phase-field model and the analytical model. (b) Velocity of the sideways motion of the a-c domain wall under static low fields. (c) (Dots) field dependence of the saturation domain wall velocity and fittings to (dashed line) $v_0^{DW} \propto E$ for $E \leq 1$ MV/m and (dash-dotted line) $v_0^{DW} \propto E^{1.3}$ for $E > 1$ MV/m. (d) (Squares) effective mass and (circles) damping coefficient of the domain wall. The gray dotted lines in (c) and (d) indicate $E = 1$ MV/m where a change in the field dependence of v_0^{DW} and α^{DW} occurs.

$$m^{DW}\frac{\partial^2 u^{DW}}{\partial t^2} + \alpha^{DW}\frac{\partial u^{DW}}{\partial t} = P_S E(t). \qquad (3)$$

Thus, the domain wall velocity under a constant field E applied from $t = 0$ is

$$v^{DW} = \frac{P_S E}{\alpha^{DW}}\left[1 - \exp\left(-\frac{\alpha^{DW}}{m^{DW}}t\right)\right], \qquad (4)$$

with a saturation velocity of $v_0^{DW} = P_S E/\alpha^{DW}$. As shown in Fig. 2(b), the time-dependent velocity under each field strength can be perfectly fitted to Eq. (4). v_0^{DW}, m^{DW}, and α^{DW} as a function of electric field are presented in Figs. 2(c)–2(d). The high-field data are obtained through fitting the simulated domain wall velocity (see Fig. S1 of the Supplemental Material [41]) before the nucleation of new domains (discussed later). While $m^{DW} \approx 0.68 \times 10^{-3}$ kg/m^2 is almost independent of the electric field, a change in the field dependence of v_0^{DW} and α^{DW} occurs at 1 MV/m. At $E \leq 1$ MV/m, $\alpha^{DW} \approx 0.5 \times 10^6$ kg/(m^2 s) is almost a constant, leading to a linear field dependence of v_0^{DW}, consistent with the experimentally reported linear field dependence range of $E = 0.2$–1.4 MV/m [49]. At $E > 1$ MV/m, α^{DW} follows $\alpha^{DW} \approx [E/(\text{MV/m})]^{-0.3} \times 0.5 \times 10^6$ kg/(m^2 s), giving rise to a nonlinear $v_0^{DW} \propto E^{1.3}$ due to an increased instability of the a domain, in

agreement with the experimentally reported field dependence of $v_0^{DW} \propto E^{1.3-1.4}$ at $E \geq 1$ MV/m for antiparallel BaTiO$_3$ domain walls [50,51].

Equation (3) can be used to predict the domain growth dynamics under an ultrafast electric-field pulse. The volume fraction of switched a domains follows

$$\Delta V^a = 2u_{Pulse}^{DW}/D, \qquad (5)$$

where D is the original a domain width, and u_{Pulse}^{DW} is the total domain wall displacement after applying the electric-field pulse, given by

$$u_{Pulse}^{DW} = \frac{P_S E T_E}{\alpha^{DW}(E)} + \frac{P_S E}{\alpha^{DW}(E)}\left(\frac{m^{DW}}{\alpha^{DW}(0)} - \frac{m^{DW}}{\alpha^{DW}(E)}\right)$$
$$\times \left[1 - \exp\left(-\frac{\alpha^{DW}(E)T_E}{m^{DW}}\right)\right], \qquad (6)$$

with the derivation provided in Note S8 of the Supplemental Material [41]. $\alpha^{DW}(E)$ and $\alpha^{DW}(0)$ are the damping coefficients under the field strength E and zero field, respectively. At $E \leq 1$ MV/m with a field-independent α^{DW}, Eq. (5) reduces to $\Delta V^a = 2P_S E T_E/(\alpha^{DW} D)$, which explains the linear dependence of ΔV^a on both pulse duration and field strength. As seen in Fig. 2(a), the low-field ΔV^a from Eq. (5) of the analytical model shows a perfect agreement with that from the phase-field model.

Upon increasing the field to $E > 2$ MV/m, 90° switching of polarization inside a domains is induced in addition to the motion of a-c domain walls. This indicates a critical field for overcoming the energy threshold for an intrinsic 90° domain switching and for inducing the instability of a domains (see Note S9 of the Supplemental Material [41]). This leads to a transition from the pure domain wall migration dynamics under low fields to the combined dynamics of domain nucleation and domain growth under high fields involving both growth of original c domains and nucleation and growth of new c domains.

The volume fraction ΔV^a of switched a domains under high fields is presented in Fig. 3(a), showing a nonlinear dependence on the pulse duration T_E. For example, at $E = 20$ MV/m, upon increasing T_E, ΔV^a first slowly increases for $T_E < 0.5$ ns and then sharply increases for $T_E > 0.5$ ns before a complete switching for $T_E = 0.8$ ns. This is due to the existence of an incubation time, $t_{incub} = 0.5$ ns, for the activation of nucleation and growth of new c domains.

The domain structure evolution under $E = 20$ MV/m with $T_E = 0.4$–0.8 ns is presented in Movies S1–S5 of the Supplemental Material [41]. For $T_E = 0.4$ ns, very few new c domains appear inside a domains, and all of them eventually shrink and vanish. This is also represented by the evolution of the average polarization $\overline{P_3}$, which eventually decreases after turning off the field [Fig. 3(b)].
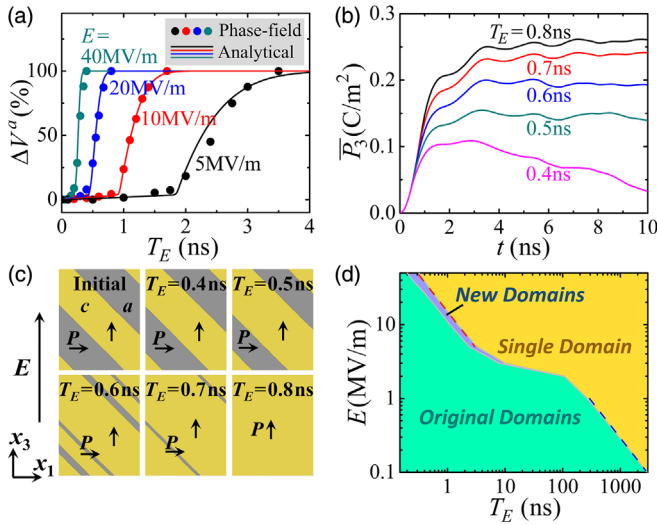
FIG. 3. (a) Volume fraction of switched a domains under high fields as a function of pulse duration, from both the phase-field model and the analytical model. (b) Evolution of the average polarization in the original a domains under electric-field pulses with $E = 20$ MV/m and different durations. (c) Initial domain structure and final domain structures after applying electric-field pulses with $E = 20$ MV/m and different durations. (d) Electric field strength—pulse duration stability diagram of the a-c domains. The red and blue dashed lines are guides to the eyes, following $ET_E = 0.015$ V s/m and $ET_E = 0.29$ V s/m, respectively.

Therefore, the structural evolution is dominated by the a-c domain wall motion. For $T_E = 0.6$–0.8 ns, new c domains nucleate inside a domains at greatly increased rates, which then expand and eventually form stable c domains, as is also shown by an increasing $\overline{P_3}$ after the field is turned off [Fig. 3(b)]. This indicates that the system gains sufficient energy out of work done by the external field to activate the nucleation of new c domains, with an energy threshold estimated to be 0.52 MJ/m^3 (see Note S10 of the Supplemental Material [41]). We also note that the nucleation is thermally activated without extrinsic effects such as defects or electrodes. The effect of a thermal field on the high-field domain dynamics is discussed in Note S11 of the Supplemental Material [41].

The activation of domain nucleation with $t_{\text{incub}} = 0.5$ ns also results in various final domain structures dependent on the pulse duration T_E. As shown in Fig. 3(c), with $T_E \leq 0.5$ ns, the original domain pattern is preserved but with displaced domain walls; for $T_E = 0.6$ ns, new c domains are formed inside the original a domains; for $T_E = 0.7$ ns, a domains start to disappear when pairs of a-c domain walls moving towards each other meet and annihilate; for $T_E \geq 0.8$ ns, all a domains are erased resulting a single c domain. Similar nanosecond domain switching through nucleation and growth of new domains under high fields was also experimentally observed [3,52].

We further show that the fraction of switched a domains under high fields can also be described analytically. Consider two contributions as follows: ΔV_1^a, the fraction of switched a domains in the case with only growth of the original domains, and ΔV_2^a, the fraction of switched a domains in the case with only nucleation and growth of new domains. Assuming that ΔV_1^a and ΔV_2^a arise from two independent processes, the combined effect can be approximated as $\Delta V^a = \Delta V_1^a + \Delta V_2^a - \Delta V_1^a \Delta V_2^a$. ΔV_1^a follows the analytical description of domain growth [Eq. (5)], where extrapolated values of α^{DW} following $\alpha^{\text{DW}} \propto E^{-0.3}$ is used for $E > 5$ MV/m. By adopting the Kolmogorov-Avrami-Ishibashi (KAI) model [53] or the nucleation-limited switching (NLS) model [54] for domain switching through nucleation and growth processes, we find that ΔV_2^a fits well to the KAI model incorporating the incubation time t_{incub} for a delayed response,

$$\Delta V_2^a = \begin{cases} 0, & T_E < t_{\text{incub}} \\ 1 - \exp\left(R v_0^{\text{DW}^n} S\right), & T_E \geq t_{\text{incub}} \end{cases},$$
$$S = (T_E - t_{\text{incub}} + r_c/v_0^{\text{DW}})^{n+1} - (r_c/v_0^{\text{DW}})^{n+1}, \quad (7)$$

with R and r_c being the nucleation rate and the critical nucleation size, respectively, and $n = 2$ the dimension of the system. r_c is given by the classical nucleation theory as $r_c = \sigma^{\text{DW}}/(P_S E)$, $\sigma^{\text{DW}} = 0.03$ J/m^2 being the domain wall energy from phase-field modeling. We take $t_{\text{incub}} \propto E^{-1}$ by assuming a critical impulse Et_{incub} that provides sufficient energy for domain nucleation.

The simulated ΔV^a from the phase-field model under high fields is fitted to the analytical model, as shown in Fig. 3(a). Values of t_{incub} and R are given in Fig. S2 of the Supplemental Material [41]. Note that for ultrafast switching dynamics, t_{incub} ($= 0.5$ ns for $E = 20$ MV/m) comprises a significant part of the whole switching process. ΔV^a from the analytical model shows a good agreement with phase-field results, validating the understanding of high-field domain dynamics as a combination of original domain growth and nucleation and growth of new domains. It is also worth noting that apart from electric fields, nucleation and growth of ferroelectric domains can also be activated by other external stimuli, e.g., heat, forces, light, currents, provided that the stimuli alter the stability of domains and provide sufficient energy to stabilize the nucleated domains. Therefore, the existence of two regimes of domain dynamics under other ultrafast stimuli with small and large magnitudes should also be expected, similar to the results reported here.

The field strength—pulse duration stability diagram of a-c domains is shown in Fig. 3(d), which summarizes three possible final domain structures after applying an electric-field pulse: (1) preservation of original a-c domain patterns with sideways displacement of domain walls at low fields and/or short pulse durations (referred to as original

domains), (2) formation of new c domains inside original a domains at high fields and intermediate pulse durations (referred to as new domains), and (3) full erasure of the a domains resulting in a single c domain at high fields and/or long pulse durations (referred to as single domain).

The boundary of single domain approximately follows a constant pulse area ET_E at both its high-field and low-field ends. The boundary between original domains and single domain at $E \leq 1$ MV/m follows $ET_E = 0.29$ V s/m from the linear field dependence of domain wall velocity. The boundary between new domains and single domain at $E \geq 5$ MV/m shows $ET_E = 0.015$ V s/m, which is determined by the field-dependent incubation time of 90° domain switching with $t_{incub} \propto E^{-1}$; similar field-dependent switching time under high electric fields was also experimentally reported very recently [52]. The transition from the low-field regime to the high-field one at around 2 MV/m is exhibited by the appearance of new domains accompanied by an abrupt shift of the phase boundary towards smaller T_E. Such a characteristic shift provides a simple way to experimentally determine the critical transition field in ferroelectric systems.

In summary, we develop a phase-field model integrating polarization dynamics and elastodynamics for studying dynamic responses of ferroelectric domains in ultrafast transient processes under ultrafast external stimuli. Simulation results reveal distinctive domain evolution mechanisms under ultrafast electric-field pulses with low ($E \leq 2$ MV/m) and high ($E > 2$ MV/m) field strengths. Analytical models are developed for describing the dynamics of domain switching and domain wall motion in both regimes. The types of new equilibrium domain structures as a function of field strength and pulse duration are predicted. The theoretical insights on electric-field-excited ultrafast domain dynamics achieved in this Letter is expected to provide useful guidance to exploring and manipulating dynamic functionalities of ferroelectric materials.

---

*tuy123@psu.edu

†lqc3@psu.edu

[1] J. Li, B. Nagaraj, H. Liang, W. Cao, C. H. Lee, and R. Ramesh, Ultrafast polarization switching in thin-film ferroelectrics, Appl. Phys. Lett. **84,** 1174 (2004).

[2] K. Takahashi, N. Kida, and M. Tonouchi, Terahertz Radiation by an Ultrafast Spontaneous Polarization Modulation of Multiferroic $BiFeO_3$ Thin Films, Phys. Rev. Lett. **96,** 117402 (2006).

[3] A. Grigoriev, D.-H. Do, D. M. Kim, C.-B. Eom, B. Adams, E. M. Dufresne, and P. G. Evans, Nanosecond Domain Wall Dynamics in Ferroelectric $Pb(Zr, Ti)O_3$ Thin Films, Phys. Rev. Lett. **96,** 187601 (2006).

[4] A. Gruverman, D. Wu, and J. F. Scott, Piezoresponse Force Microscopy Studies of Switching Behavior of Ferroelectric Capacitors on a 100-ns Time Scale, Phys. Rev. Lett. **100,** 097601 (2008).

[5] D. S. Rana, I. Kawayama, K. Mavani, K. Takahashi, H. Murakami, and M. Tonouchi, Understanding the nature of ultrafast polarization dynamics of ferroelectric memory in the multiferroic $BiFeO_3$, Adv. Mater. **21,** 2881 (2009).

[6] K.-J. Jang, H.-g. Lee, S. Lee, J. Ahn, J. S. Ahn, N. Hur, and S.-W. Cheong, Strong spin-lattice coupling in multiferroic hexagonal manganite $YMnO_3$ probed by ultrafast optical spectroscopy, Appl. Phys. Lett. **97,** 031914 (2010).

[7] D. Daranciang *et al.*, Ultrafast Photovoltaic Response in Ferroelectric Nanolayers, Phys. Rev. Lett. **108,** 087601 (2012).

[8] L. Y. Chen, J. C. Yang, C. W. Luo, C. W. Laing, K. H. Wu, J.-Y. Lin, T. M. Uen, J. Y. Juang, Y. H. Chu, and T. Kobayashi, Ultrafast photoinduced mechanical strain in epitaxial $BiFeO_3$ thin films, Appl. Phys. Lett. **101,** 041902 (2012).

[9] Y. M. Sheu, S. A. Trugman, L. Yan, Q. X. Jia, A. J. Taylor, and R. P. Prasankumar, Using ultrashort optical pulses to couple ferroelectric and ferromagnetic order in an oxide heterostructure, Nat. Commun. **5,** 5832 (2014).

[10] C. v. Korff Schmising, M. Bargheer, M. Kiel, N. Zhavoronkov, M. Woerner, T. Elsaesser, I. Vrejoiu, D. Hesse, and M. Alexe, Coupled Ultrafast Lattice and Polarization Dynamics in Ferroelectric Nanolayers, Phys. Rev. Lett. **98,** 257601 (2007).

[11] H. Akamatsu, Y. Yuan, V. A. Stoica, G. Stone, T. Yang, Z. Hong, S. Lei, Y. Zhu, R. C. Haislmaier, J. W. Freeland, L.-Q. Chen, H. Wen, and V. Gopalan, Light-Activated Gigahertz Ferroelectric Domain Dynamics, Phys. Rev. Lett. **120,** 096101 (2018).

[12] R. Mankowsky, A. von Hoegen, M. Forst, and A. Cavalleri, Ultrafast Reversal of the Ferroelectric Polarization, Phys. Rev. Lett. **118,** 197601 (2017).

[13] V. A. Stoica, N. Laanait, C. Dai, Z. Hong, Y. Yuan, Z. Zhang, S. Lei, M. R. McCarter, A. Yadav, A. R. Damodaran, S. Das, G. A. Stone, J. Karapetrova, D. A. Walko, X. Zhang, L. W. Martin, R. Ramesh, L.-Q. Chen, H. Wen, V. Gopalan, and J. W. Freeland, Optical creation of a supercrystal with three-dimensional nanoscale periodicity, Nat. Mater. **18,** 377 (2019).

[14] H. Wen, P. Chen, M. P. Cosgriff, D. A. Walko, J. H. Lee, C. Adamo, R. D. Schaller, J. F. Ihlefeld, E. M. Dufresne, D. G. Schlom, P. G. Evans, J. W. Freeland, and Y. Li, Electronic origin of ultrafast photoinduced strain in $BiFeO_3$, Phys. Rev. Lett. **110,** 037601 (2013).

[15] M. Lejman, G. Vaudel, I. C. Infante, P. Gemeiner, V. E. Gusev, B. Dkhil, and P. Ruello, Giant ultrafast photo-induced shear strain in ferroelectric $BiFeO_3$, Nat. Commun. **5,** 4301 (2014).

[16] Y. Qi, S. Liu, A. M. Lindenberg, and A. M. Rappe, Ultrafast Electric Field Pulse Control of Giant Temperature Change in Ferroelectrics, Phys. Rev. Lett. **120,** 055901 (2018).

[17] C. Kittel, Domain boundary motion in ferroelectric crystals and the dielectric constant at high frequency, Phys. Rev. **83,** 458 (1951).

[18] J. Fousek and B. Brezina, Relaxation of 90 degrees domain walls of BaTiO$_3$ and their equation of motion, J. Phys. Soc. Jpn. **19**, 830 (1964).

[19] G. Arlt and N. A. Pertsev, Force constant and effective mass of 90 degrees domain walls in ferroelectric ceramics, J. Appl. Phys. **70**, 2283 (1991).

[20] S. Li, W. Cao, and L. E. Cross, The extrinsic nature of nonlinear behavior observed in lead zirconate titanate ferroelectric ceramic, J. Appl. Phys. **69**, 7219 (1991).

[21] G. Arlt, U. Bttger, and S. Witte, Emission of GHz shear waves by ferroelastic domain walls in ferroelectrics, Appl. Phys. Lett. **63**, 602 (1993).

[22] M. D. Glinchuk, E. A. Eliseev, and V. A. Stephanovich, Dynamical dielectric susceptibility of ferroelectric thin films and multilayers, Phys. Solid State **44**, 953 (2002).

[23] A. Q. Jiang, H. J. Lee, C. S. Hwang, and J. F. Scott, Subpicosecond processes of ferroelectric domain switching from field and temperature experiments, Adv. Funct. Mater. **22**, 192 (2012).

[24] I. Katayama, H. Aoki, J. Takeda, H. Shimosato, M. Ashida, R. Kinjo, I. Kawayama, M. Tonouchi, M. Nagai, and K. Tanaka, Ferroelectric Soft Mode in a SrTiO$_3$ Thin Film Impulsively Driven to the Anharmonic Regime Using Intense Picosecond Terahertz Pulses, Phys. Rev. Lett. **108**, 097401 (2012).

[25] A. Subedi, Proposal for ultrafast switching of ferroelectrics using midinfrared pulses, Phys. Rev. B **92**, 214303 (2015).

[26] Y.-H. Shin, I. Grinberg, I.-W. Chen, and A. M. Rappe, Nucleation and growth mechanism of ferroelectric domain-wall motion, Nature (London) **449**, 881 (2007).

[27] I. Ponomareva, L. Bellaiche, T. Ostapchuk, J. Hlinka, and J. Petzelt, Terahertz dielectric response of cubic BaTiO$_3$, Phys. Rev. B **77**, 012102 (2008).

[28] I. Grinberg, Y.-H. Shin, and A. M. Rappe, Molecular Dynamics Study of Dielectric Response in a Relaxor Ferroelectric, Phys. Rev. Lett. **103**, 197601 (2009).

[29] T. Qi, Y.-H. Shin, K.-L. Yeh, K. A. Nelson, and A. M. Rappe, Collective Coherent Control: Synchronization of Polarization in Ferroelectric PbTiO$_3$ by Shaped THz Fields, Phys. Rev. Lett. **102**, 247603 (2009).

[30] D. Wang, J. Weerasinghe, L. Bellaiche, and J. Hlinka, Dynamical coupling in Pb(Zr, Ti)O$_3$ solid solutions from first principles, Phys. Rev. B **83**, 020301(R) (2011).

[31] Q. Zhang, R. Herchig, and I. Ponomareva, Nanodynamics of Ferroelectric Ultrathin Films, Phys. Rev. Lett. **107**, 177601 (2011).

[32] K. McCash, A. Srikanth, and I. Ponomareva, Competing polarization reversal mechanisms in ferroelectric nanowires, Phys. Rev. B **86**, 214108 (2012).

[33] Z. Gui and L. Bellaiche, Terahertz dynamics of ferroelectric vortices from first principles, Phys. Rev. B **89**, 064303 (2014).

[34] R. Xu, S. Liu, I. Grinberg, J. Karthik, A. R. Damodaran, A. M. Rappe, and L. W. Martin, Ferroelectric polarization reversal via successive ferroelastic transitions, Nat. Mater. **14**, 79 (2015).

[35] S. Liu, I. Grinberg, and A. M. Rappe, Intrinsic ferroelectric switching from first principles, Nature (London) **534**, 360 (2016).

[36] E. K. H. Salje, X. Wang, X. Ding, and J. F. Scott, Ultrafast switching in avalanche-driven ferroelectrics by supersonic kink movements, Adv. Funct. Mater. **27**, 1700367 (2017).

[37] B. Xu, V. Garcia, S. Fusil, M. Bibes, and L. Bellaiche, Intrinsic polarization switching mechanisms in BiFeO$_3$, Phys. Rev. B **95**, 104104 (2017).

[38] L.-Q. Chen, Phase-field method of phase transitions/domain structures in ferroelectric thin films: A review, J. Am. Ceram. Soc. **91**, 1835 (2008).

[39] H. L. Hu and L.-Q. Chen, Three-dimensional computer simulation of ferroelectric domain formation, J. Am. Ceram. Soc. **81**, 492 (1998).

[40] S. Nambu and D. A. Sagala, Domain formation and elastic long-range interaction in ferroelectric perovskites, Phys. Rev. B **50**, 5838 (1994).

[41] See the Supplemental Material at http://link.aps.org/supplemental/10.1103/PhysRevLett.124.107601 for numerical solutions to dynamical phase-field equations, comparisons of relaxational and dynamical models, derivations and parameters of the analytical models, and supporting figures and movies.

[42] Y. Li, L. E. Cross, and L.-Q. Chen, A phenomenological thermodynamic potential for BaTiO$_3$ single crystals, J. Appl. Phys. **98**, 064101 (2005).

[43] Y. Li, S. Y. Hu, Z.-K. Liu, and L.-Q. Chen, Effect of substrate constraint on the stability and evolution of ferroelectric domain structures in thin films, Acta Mater. **50**, 395 (2002).

[44] L.-Q. Chen and J. Shen, Applications of semi-implicit Fourier-spectral method to phase field equations, Comput. Phys. Commun. **108**, 147 (1998).

[45] S. Y. Hu and L.-Q. Chen, A phase-field model for evolving microstructures with strong elastic inhomogeneity, Acta Mater. **49**, 1879 (2001).

[46] J. Wang, X. Ma, Q. Li, J. Britson, and L.-Q. Chen, Phase transitions and domain structures of ferroelectric nanoparticles: Phase field model incorporating strong elastic and dielectric inhomogeneity, Acta Mater. **61**, 7591 (2013).

[47] K. Tani, Dynamics of displacive-type ferroelectrics –soft modes–, J. Phys. Soc. Jpn. **26**, 93 (1969).

[48] A. K. Bandyopadhyay, P. C. Ray, and G. Venkatraman, An approach to the Klein-Gordon equation for a dynamic study in ferroelectric materials, J. Phys. Condens. Matter **18**, 4093 (2006).

[49] W. J. Merz, Domain formation and domain wall motions in ferroelectric BaTiO$_3$ single crystals, Phys. Rev. **95**, 690 (1954).

[50] H. Stadler, Ferroelectric switching time of BaTiO$_3$ crystals at high voltages, J. Appl. Phys. **29**, 1485 (1958).

[51] H. Stadler and P. Zachmanidis, Nucleation and growth of ferroelectric domains in BaTiO$_3$ at fields from 2 to 450 kV/cm, J. Appl. Phys. **34**, 3255 (1963).

[52] H. J. Lee, T. Shimizu, H. Funakubo, Y. Imai, O. Sakata, S. H. Hwang, T. Y. Kim, C. Yoon, C. Dai, L.-Q. Chen, S. Y. Lee, and J. Y. Jo, Electric-Field-Driven Nanosecond Ferroelastic-Domain Switching Dynamics in Epitaxial Pb(Zr, Ti)O$_3$ Film, Phys. Rev. Lett. **123**, 217601 (2019).

[53] Y. Ishibashi and Y. Takagi, Note on ferroelectric domain switching, J. Phys. Soc. Jpn. **31**, 506 (1971).

[54] A. K. Tagantsev, I. Stolichnov, N. Setter, J. S. Cross, and M. Tsukada, Non-Kolmogorov-Avrami switching kinetics in ferroelectric thin films, Phys. Rev. B **66**, 214109 (2002).